

Alternate Thermoelectric Thermodynamic Cycles with Improved Power Generation Efficiencies

Lon E. Bell, PhD
 BSST, LLC
 5462 Irwindale Avenue, Irwindale CA 91706
 lbell@amerigon.com, 626.815.7430

Abstract

Solid-state power generation has not seen broad application because energy conversion efficiency has been too low to justify the expense of such systems, or because competing technologies offer better efficiencies. Alternate thermodynamic cycles compatible with thermoelectric systems offer the promise of substantially higher efficiency, while the configurations of such systems exhibit high power densities as an attendant benefit. These cycles offer significant improvements in the efficiency of power extraction from hot fluid streams, such as in conditions associated with automotive exhaust, catalytic combustors, and co-cycle power generators. In this paper, several cycles are analyzed to determine their suitability for particular classes of application and their relative efficiencies.

Terminology

\dot{M} = mass flow rate of convective medium (kg/s)
 C_p = specific heat of convective medium (J/kgK)
 T_C = fixed cold side temperature (K)
 T_H = fixed hot side temperature (K)
 $T_{iC}(x)$ = cold side temperature at position x (K)
 $T_{iH}(x)$ = hot side temperature at position x (K)
 T_G = bulk temperature of convective medium (K)
 P_i = electrical power output (W)
 $p(x)$ = electrical power output at position x (W/cm)
 Q_{iC} = total cold side thermal flux (W)
 $q_{iC}(x)$ = cold side thermal flux at position x (W/cm)
 Q_{iH} = total hot side thermal flux (W)
 $q_{iH}(x)$ = hot side thermal flux at position x (W/cm)
 T_{iM}, T_{iMC}, T_{iMH} = intermediate temperatures (K)
 β = dimensionless thermal mass ratio
 η = fixed dimensionless material efficiency parameter
 α = Seebeck coefficient (V/K)
 λ = thermal conductivity (W/cmK)
 ρ = electrical resistivity ($\Omega\text{-cm}$)

Subscripts

j = property associated with configuration j
 C = property at cold side of system
 G = external property
 H = property at hot side of system
 M = intermediate property

Introduction

Recent advancements in thermoelectric (TE) materials [1, 2] and systems [3-5] have renewed interest in the potential use of TEs for power generation. The inherent qualities of TE systems: few if any moving parts, quiet operation and

prospects of both environmental friendliness and waste power recovery, have further increased the interest.

Texts that describe solid-state TE power generation were either written contemplating spacecraft usage, concerned with terrestrial applications for which reliability rather than efficiency has been the primary goal or used formulaic models that do not necessarily optimize system performances for today's applications. [6] The need exists to look comprehensively at TE power generation with special emphasis on factors that influence efficiency, including appropriate hot and cold side boundary conditions, use of recently developed thermodynamic cycles and newer TE materials. The source of thermal power (heat) and the available means of eliminating waste heat from the cold side are shown to strongly influence efficiency. Maintaining high efficiency in fluidic systems is the primary subject of this paper. Other factors, such as system complexity, durability and cost, have a large effect on efficiency, and are discussed briefly here, but not in sufficient detail to be fully applicable.

The analysis that follows is separated into four general categories in accordance with the nature of the hot and cold side boundary conditions. The most commonly used boundary conditions assume that both the hot and cold sides are isotropic at temperatures T_H and T_C , respectively. These conditions, designated as Configuration 1, are used in most texts, but are rarely achievable in practical power generation applications. Subsequent configurations replace one or both of the isotropic boundaries with convective media as sources and sinks for thermal power. These boundary conditions are more common in today's applications. Property changes related to the thermoelectric figure of merit, Z , vary as discussed at appropriate points in this paper. All other material properties, such as heat capacity and thermal conductivity, are postulated as independent of temperature and time. Figure 1A gives a schematic of a typical TE couple operating as a power generator. Thermal power enters the hot side of a TE couple at temperature T_H . The opposite end of the TE couple is maintained at a colder temperature T_C . The temperature difference $T_H - T_C$ induces a conductive thermal flux, Q_{iH} , from the hot to the cold side. The thermoelectric properties of the couple, the heat flux and ΔT determine the amount of electrical power P_i produced and waste heat flux Q_{iC} that exits the cold side. Conservation of energy, in steady-state operation, requires that;

$$Q_{iH} - Q_{iC} = P_i \quad (1)$$

where P_i is the electric power produced. Maximum efficiency, P_i , is given by;

$$\frac{P_i}{Q_{iH}} = \left(\frac{T_H - T_C}{T_H} \right) \left(1 + \frac{2(\sqrt{ZT_{AVE}} + 1)}{ZT_H} \right)^{-1} \quad (2)$$

Where;

$$Z = \frac{\alpha}{\lambda p} \quad (3)$$

$$T_{AVE} = \frac{T_H + T_C}{2} \quad (4)$$

To simplify the analysis without distorting the relative performance of the configurations studied, the following simplifying assumptions are made. The first term on the right hand side is the Carnot efficiency, and the second term is a material factor associated with a thermoelectric generator. This factor will appear frequently in the computations that follow and is designated by η ;

$$\eta = \left(1 + \frac{2(\sqrt{ZT_{AVE} + 1} + 1)}{ZT_H} \right)^{-1} \quad (5)$$

It is a measure of TE material properties and the TE geometry of Figure 1A. It is assumed to vary only with the ZT_H of the TE material. Its variation with T_{AVE} is ignored, as the error induced by doing so is very small for the parameter range in this paper.

Equation (2) will be used, with a range of boundary conditions, to compute the efficiency of TE elements in various generator configurations. Basic cases are classified as to whether the hot side is an infinite heat source at T_H or a working fluid initially at temperature T_G . Similarly, the cold side is either an infinite heat sink at T_C or a working fluid initially at temperature T_C . The four general conditions are summarized in Table 1. In the analysis that follows, the four boundary conditions identified in Table 1 are further broken into a total of twelve configurations. Results for each are presented, and where appropriate, approximate formulas for estimating performance are given.

Boundary Condition	Systems	Configuration Numbers
Hot Side Infinite Heat Source	Isotope; solar; reactor heat source; intermediate stage of a TE element cascade; hot side of a low power system.	1, 3, 6
Hot Side Working Fluid	Hot working fluid such as combustion products; hot exhaust gases; steam; heat exchanger; process flow fluids	2, 4, 5, 7, 8, 9, 10, 11, 12
Cold Side Infinite Heat Sink	Stage of TE element cascade; large thermal reservoir such as ocean water; space craft; aircraft skin; cold side of low power system	1, 2, 7, 11
Cold Side Working Fluid	Forced air or liquid cooling system; radiator; passive cooling; heat exchanger; process systems	3, 4, 5, 6, 8, 9, 10, 12

Table 2

Typical systems that have the boundary conditions denoted in Table 1 are presented in Table 2. Generally, low power systems such as those used in instrumentation, or signal generation have constant temperature (effectively infinite heat sources and sinks). Waste heat, exhaust and combustion

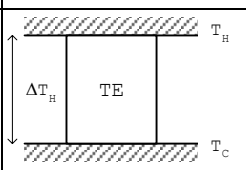
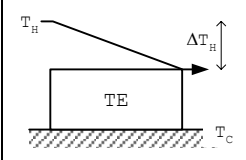
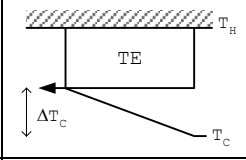
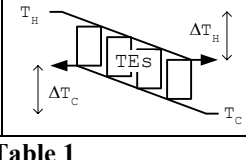
Hot Side	Cold Side	Conditions	Configuration Numbers
Infinite Heat Source	Infinite Heat Sink		1
Working Fluid	Infinite Heat Sink		2, 7, 11
Infinite Heat Source	Working Fluid		3, 6
Working Fluid	Working Fluid		4, 5, 8, 9, 10, 12

Table 1

powered generators have working fluids as heat sources, in which the initial fluid peak temperature, T_G , is equal to, or higher than the maximum operating temperature of the TE.

Under certain important conditions, for example, when the temperature difference between the hot and cold side is very large, it is known to be advantageous to segment materials in TE generator couples [6], and in doing so, incorporate the material that exhibits the highest possible ZT for each particular temperature range.

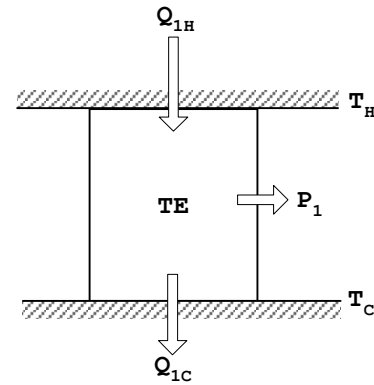


Figure 1A

Configuration 1

This system consists of a hot side heat source that delivers thermal power Q_{1H} at a uniform temperature T_H . Similarly, the cold side is in contact with a heat sink Q_{1C} at uniform temperature T_C . The solid-state energy converter is defined in terms of uniform material property Z . The system operates under steady state conditions and constant TE properties. Electrical power produced by the hot side thermal flux Q_{1H} ,

across the temperature difference $T_H - T_C$ is defined as P_1 . For this configuration, the optimum efficiency can be written as the Carnot efficiency, $(T_H - T_C) / T_H$, times the material term η , defined in Equation (5);

$$\frac{P_1}{Q_{1H}} = \left(\frac{T_H - T_C}{T_H} \right) \eta \quad (6)$$

This is a well-known result. [6] Figure 1B presents a graph of the calculated efficiency using Equation (6) for the hot to cold side temperature ratio ranging from 0 to 1. Computations for various values of ZT_H are given. The lowest, $ZT_H = 1$ is representative of today's best commercial material and $ZT_H = 2.5$ is the highest reported value in current literature. [1]

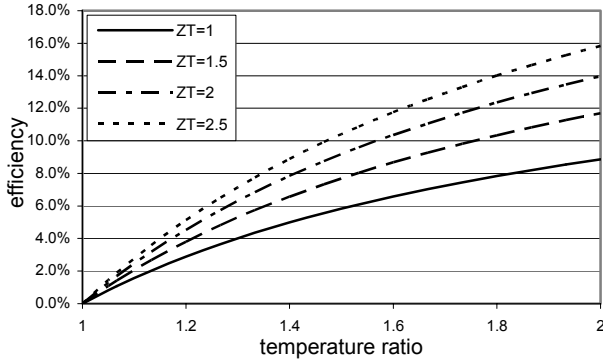


Figure 1B

Configuration 2

Configuration 2 is shown in Figure 2A. In this geometry, the hot side thermal flux Q_{2H} is contained in a convective medium with temperature independent properties;

$$Q_{2H} = (T_H - T_C) C_P \dot{M} \quad (7)$$

where $C_P \dot{M}$ = thermal inertia.

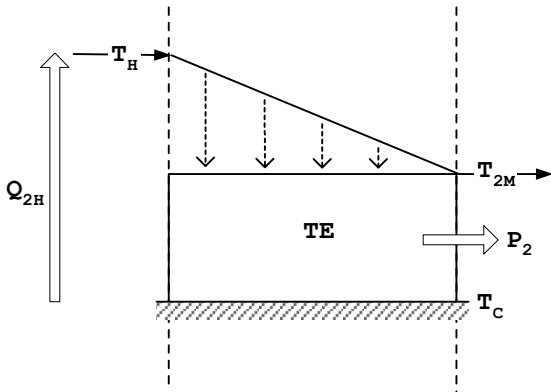


Figure 2A

The heat content associated with increasing a given amount of the medium to temperature T_H from T_C is Q_{2H} . The energy converter operates between T_{2M} and T_C . The portion of Q_{2H} passing through the TE system, Q_{2E} , is;

$$Q_{2E} = (T_H - T_{2M}) C_P \dot{M} \quad (8)$$

The balance is not utilized in the conversion process and exits as waste heat flux Q_{2W} . All of the thermal power

Q_{2E} enters the hot side of the TE converter at uniform temperature T_{2M} .

Temperature T_{2M} is that temperature which optimizes system efficiency. T_{2M} is calculated by noting that;

$$\frac{P_2}{Q_{2H}} = \frac{Q_{2E}}{Q_{2H}} \frac{(T_{2M} - T_C)}{T_{2M}} \eta \quad (9)$$

$$= \frac{(T_H - T_{2M})(T_{2M} - T_C)}{(T_H - T_C) T_{2M}} \eta \quad (10)$$

By the assumptions made, the product ZT_{2M} is a constant and not a function of T_{2M} . Similarly, it is assumed that the term $\sqrt{ZT_{AVE} + 1}$ from Equation (2) is constant. This is not an approximation to the extent that the TE material can be tailored to have the specified value for ZT_H regardless of what T_H is.

Equation (10) is maximized with respect to T_{2M} , if;

$$T_{2M} = \sqrt{T_H T_C} \quad (11)$$

Figure 2B presents results for Configuration 2 for T_H / T_C ranging from 1.0 to 2.0 for four values of ZT_H .

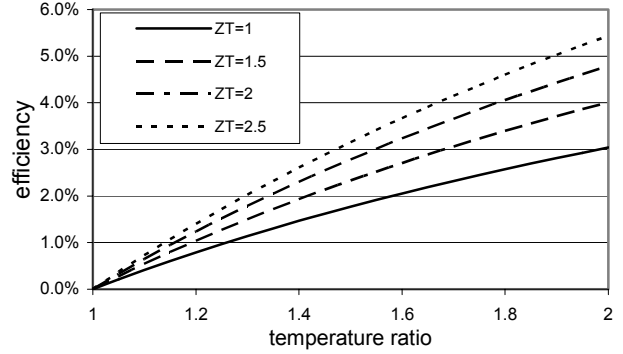


Figure 2B

Configuration 3

Configuration 3 is shown in Figure 3A. It is similar to Configuration 2, except that the hot side is at uniform temperature T_H and the cold side is cooled by a fluid with flow rate \dot{M} such that the medium's heat capacity equals Q_{3H} .

If the flow rate, and thus the heat capacity, of the cold side is not constrained, efficiency monotonically increases to that of Configuration 1, since at very high waste side flow rates, $T_{3M} \rightarrow T_C$, and the efficiency of Equation (6) is approached. To differentiate Configuration 3 from

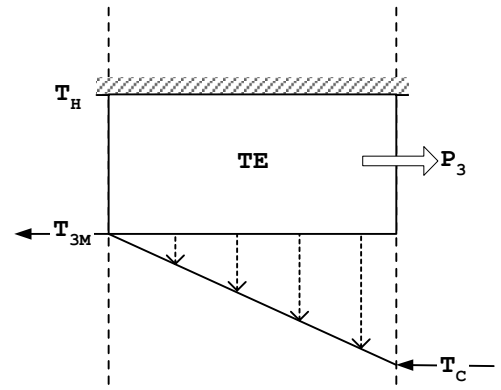


Figure 3A

Configuration 1, a representative limit can be placed on the cold side thermal capacity Q_{3C} . An obvious choice is to equate Q_{3C} to the amount of thermal power required to heat the cold side coolant from T_C to T_H ;

$$Q_{3C} = (T_H - T_C) C_P \dot{M} \quad (12)$$

This optimum efficiency will occur as $Q_{3H} \rightarrow 0$ and $T_{3M} \rightarrow T_C$ as noted above. However, if the coolant flow is restricted to that flow rate given by Equation (12), electric power output P_{3M} does have a maximum.

Since;

$$P_3 = Q_{3H} \left(\frac{T_H - T_{3M}}{T_H} \right) \eta \quad (13)$$

and;

$$Q_{3H} = (T_H - T_C) C_P \dot{M} + P_3 \quad (14)$$

Using Equations (14) in (13);

$$P_3 = (P_3 + (T_{3M} - T_C) C_P \dot{M}) \left(\frac{T_H - T_{3M}}{T_H} \right) \eta \quad (15)$$

$$P_3 = \eta C_P \dot{M} \frac{(T_{3M} - T_C)(T_H - T_{3M})}{(1 - \eta) T_H + \eta T_{3M}} \quad (16)$$

The maximum power is found by maximizing P_3 with respect to T_{3M} . The result for T_{3M} is;

$$T_{3M} = \frac{T_H}{\eta} \left[\eta - 1 + \sqrt{(1 - \eta) + \eta \frac{T_C}{T_H}} \right] \quad (17)$$

The efficiency at maximum power output is;

$$\frac{P_{3MAX}}{Q_{3H}} = \frac{P_{3MAX}}{P_{3MAX} + Q_{3C}} = \eta \frac{T_H - T_{3M}}{T_H} \quad (18)$$

Using the value for T_{3M} from Equation (17), (18) can be evaluated. The maximum power output is given in Figure 3B.

Configuration 4

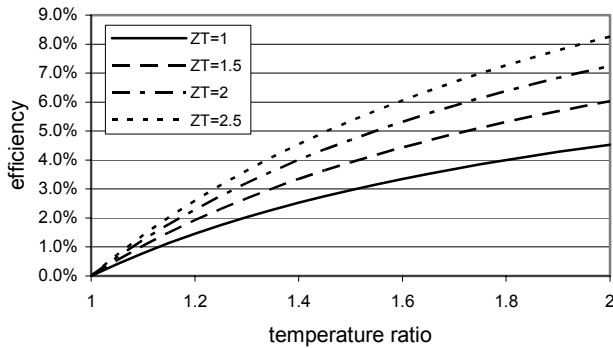


Figure 3B

Configuration 4 is pictured in Figure 4A. It is similar to Configurations 2 and 3 in that the heat flux resides in convective medium, and a second convective medium has been added. Here, the condition imposed is that the cold and hot side media have the same thermal capacities. For the hot and cold sides of the TE, each at uniform temperatures T_{4MH} and T_{4MC} , the following equations apply;

$$Q_{4MH} = (T_H - T_{4MH}) C_P \dot{M} \quad (19)$$

$$Q_{4MC} = (T_{4MC} - T_C) C_P \dot{M} \quad (20)$$

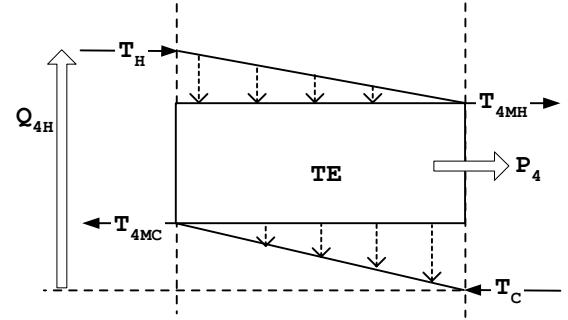


Figure 4A

$$Q_{4MH} = Q_{4MC} + P_4 \quad (21)$$

$$Q_{4H} = (T_H - T_C) C_P \dot{M} \quad (22)$$

The efficiency is;

$$\frac{P_4}{Q_{4H}} = \frac{Q_{4MH}}{Q_{4H}} \eta \frac{(T_{4MH} - T_{4MC})}{T_{4MH}} \quad (23)$$

Using Equations (19) and (22) in (23);

$$\frac{P_4}{Q_{4H}} = \frac{(T_{4MH} - T_{4MC})}{T_{4MH}} \eta \left(\frac{T_H - T_{4MH}}{T_H - T_C} \right) \quad (24)$$

The optimum efficiency can be found by writing T_{4MC} in terms of T_{4MH} , and using Equations (19) to (22);

$$T_{4MH} = T_{4MC} \frac{(1 - \eta)(T_H - T_{4MC}) + T_C}{(1 + \eta)T_{4MC} - \eta T_H} \quad (25)$$

The optimum efficiency can be found numerically from Equations (24) and (25). A useful approximate solution is found by noting that, for low efficiencies;

$$Q_{4H} \approx Q_{4C} \quad (26)$$

So that;

$$T_H - T_{4MH} \approx T_{4MC} - T_C \quad (27)$$

Or;

$$T_{4MH} = T_H + T_C - T_{4MC} \quad (28)$$

Using this in Equation (24);

$$\frac{P_4}{Q_{4H}} \approx 2\eta \frac{(\sqrt{T_H} - \sqrt{T_A})^2}{T_H - T_C} \quad (29)$$

Where;

$$T_A = \frac{T_H + T_C}{2} \quad (30)$$

Numerical results for and the approximations from Equation (29) are presented in Figure 4B.

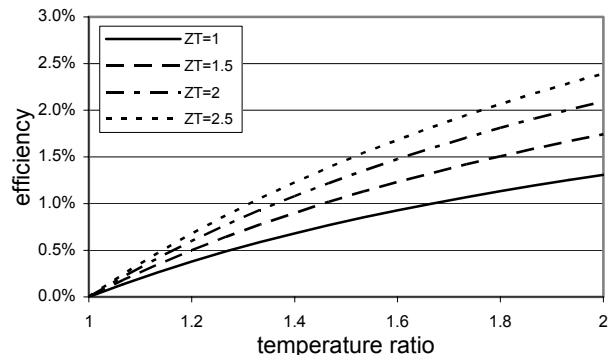


Figure 4B

Configuration 5

Configuration 5 is very similar to Configuration 4 with the exception the cold side medium that has been heated to T_{5MC} by the TE, is heated further to T_H and used as the hot side medium, as shown in Figure 5A.

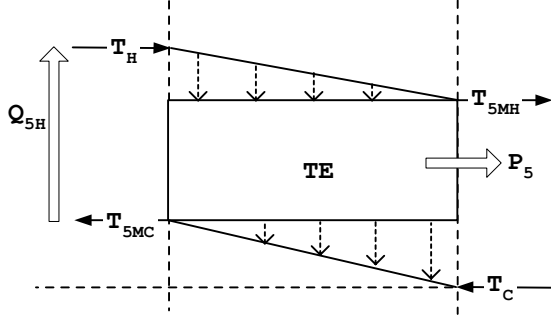


Figure 5A

In this case, the power input Q_{5H} becomes;

$$Q_{5H} = (T_H - T_{5MC}) C_P \dot{M} \quad (31)$$

And the efficiency is;

$$\frac{P_5}{Q_{5H}} = \left(\frac{T_H - T_{5MH}}{T_H - T_{5MC}} \right) \left(\frac{T_{5MH} - T_{5MC}}{T_{5MH}} \right) \eta \quad (32)$$

In addition to Equation (31), the energy balance equations are;

$$Q_{5C} = (T_{5MC} - T_C) C_P \dot{M} \quad (33)$$

And;

$$Q_{5H} - Q_{5C} = P_5 \quad (34)$$

Solving Equations (31) to (34) for T_{5MH} in terms of T_{5MC} yields;

$$T_{5MH} = T_{5MC} \frac{(1-\eta)(T_H - T_{5MC}) + T_C}{(1+\eta)T_{5MC} - \eta T_H} \quad (35)$$

Equation (35) is used in Equation (32) to find numerically the optimum value of the efficiency. Results are presented in Figure 5B.

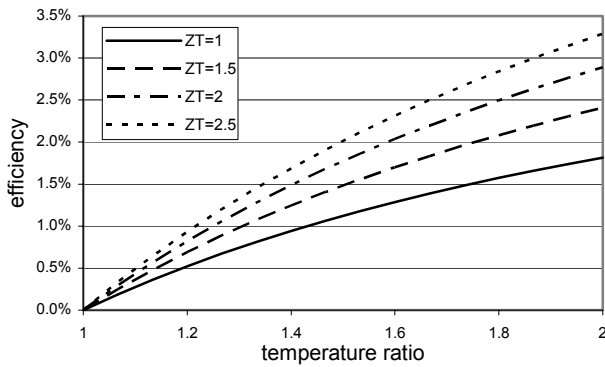


Figure 5B

Configuration 6

Configuration 6 is a generator of the type shown in Figure 6A. It is characterized by a constant hot side temperature T_H for which a cold side convective medium provides heat. The TE power generator consists of a continuous array of TE elements thermally isolated from each other in the x direction. $q_{6C}(x)$, the thermal flux into the cold side is thus;

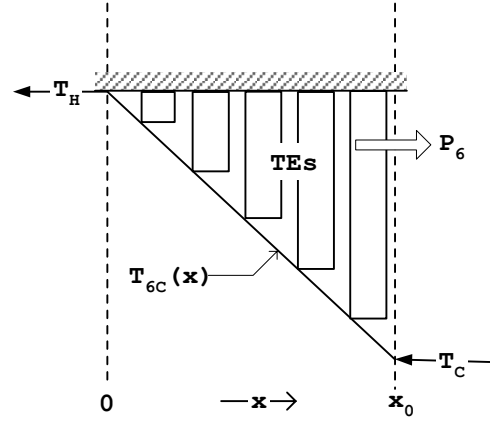


Figure 6A

$$q_{6C}(x) = C_P \dot{M} \frac{dT_{6C}(x)}{dx} \quad (36)$$

Where $T_{6C}(x)$ is the cold side medium temperature at x . Choose $T_{6C}(x)$ to be linear. Then;

$$T_{6C}(x) = T_{6C}(0) + (T_H - T_C) \frac{x}{x_0} = T_C + (T_H - T_C) \frac{x}{x_0} \quad (37)$$

And;

$$q_{6C}(x) = C_P \dot{M} \frac{dT_{6C}(x)}{dx} = \frac{C_P \dot{M} (T_H - T_C)}{x_0} \quad (38)$$

The corresponding flux from the heat source at temperature T_H is;

$$q_{6H}(x) = q_{6C}(x) + p_6(x) \quad (39)$$

where $q_{6H}(x)$ is the hot side thermal flux at x and $p_6(x)$ is the power produced at x ;

$$p_6(x) = q_{6H}(x) \eta \left(\frac{T_H - T_{6C}(x)}{T_H} \right) \quad (40)$$

The maximum efficiency is the integral of the optimal power production at each location x $p_6(x)$ divided by the integral of the power in q_{6H} ;

$$\frac{P_6}{Q_{6H}} = \frac{\int_0^{x_0} p_6(x) dx}{\int_0^{x_0} q_{6H}(x) dx} \quad (41)$$

Using Equation (39) for $q_{6H}(x)$;

$$\frac{P_6}{Q_{6H}} = \frac{\int_0^{x_0} P_{6C}(x) dx}{C_P \dot{M} (T_H - T_C) + \int_0^{x_0} P_{6C}(x) dx} \quad (42)$$

Substitution of Equations (37) to (39) into Equation (40) yields;

$$P_6 = q_{6C} \frac{\eta (T_H - T_C)}{T_H} \int_0^{x_0} \frac{1 - \frac{x}{x_0}}{1 - \frac{\eta (T_H - T_C)}{T_H}} dx \quad (43)$$

$$= q_{6C} \left(1 + \frac{\ln \left(1 - \frac{\eta (T_H - T_C)}{T_H} \right)}{\frac{\eta (T_H - T_C)}{T_H}} \right) \quad (44)$$

And the maximum efficiency from Equation (44) is;

$$\frac{P_6}{Q_{6H}} = \frac{1 - \frac{\eta(T_H - T_C)}{T_H}}{\ln\left(1 - \frac{\eta(T_H - T_C)}{T_H}\right)} \quad (45)$$

This result can be approximated by expanding the logarithmic term. A convenient approximation is;

$$\frac{P_6}{Q_{6H}} \approx \frac{\eta}{2} \left(\frac{T_H - T_C}{T_H} \right) \left(1 + \frac{\eta(T_H - T_C)}{6T_H} \right) \quad (46)$$

Results of Equations (45) and (46) are given in Figure 6B.

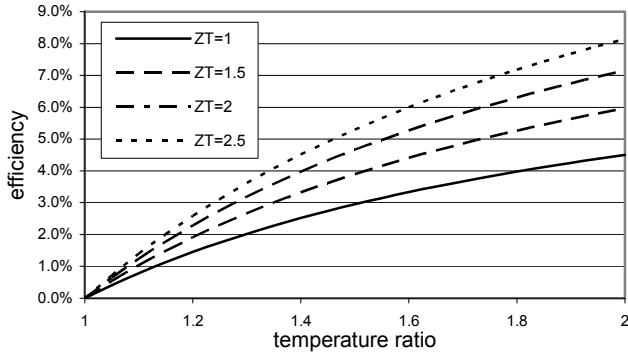


Figure 6B

Configuration 7

Configuration 7 is shown in Figure 7A. It is similar to Configuration 6, except the hot side utilizes a convective medium and the cold side is a constant temperature heat sink. The TE generator at x operates between $T_{7H}(x)$ and T_C and each is thermally isolated from other TE generators in the x direction. Computations follow those of the previous case. Imposing the condition that $T_{7H}(x)$ is linear yields;

$$T_{7H}(x) = T_H - (T_H - T_C) \frac{x}{x_0} \quad (47)$$

So that $q_{7H}(x)$ becomes;

$$q_{7H}(x) = C_P \dot{M} \frac{dT_{7H}(x)}{dx} - C_P \dot{M} \frac{(T_H - T_C)}{x_0} \quad (48)$$

and;

$$p_7(x) = \eta q_{7H} \left(\frac{T_{7H}(x) - T_C}{T_{7H}(x)} \right) \quad (49)$$

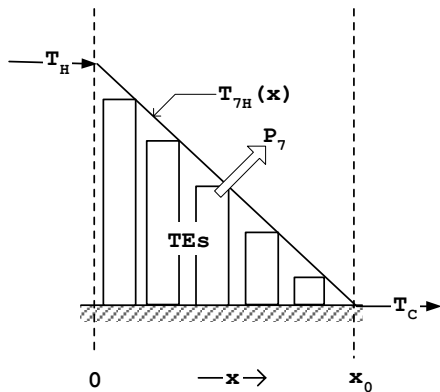


Figure 7A

The maximum efficiency is;

$$\frac{P_7}{Q_{7H}} = \frac{\int_0^{x_0} q_{7H}(x) \eta \left(\frac{T_{7H}(x) - T_C}{T_{7H}(x)} \right) dx}{\int_0^{x_0} q_{7H}(x) dx} \quad (50)$$

Integration yields;

$$\frac{P_7}{Q_{7H}} = \eta \left(1 - \frac{T_C}{T_H - T_C} \ln \frac{T_H}{T_C} \right) \quad (51)$$

Results are given in Figure 7B.

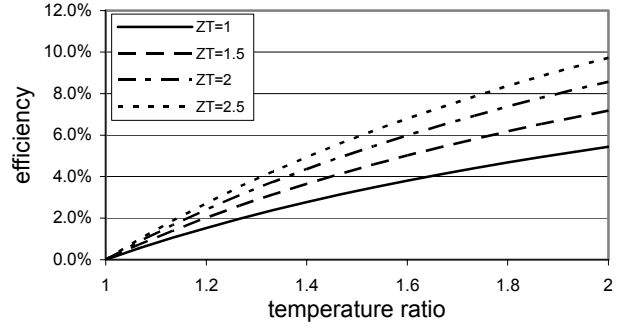


Figure 7B

Configuration 8

Configuration 8 is shown in Figure 8A. Again, in this geometry, thermal isolation in the x direction is employed. The hot side medium convects thermal power $q_{8H}(x)$ to the TEs at a constant rate so that $T_{8H}(x)$ is linear;

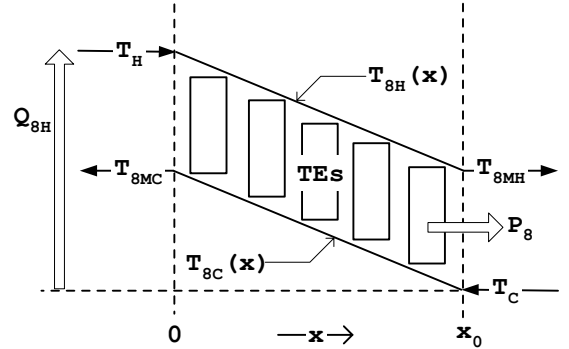


Figure 8A

$$T_{8H}(x) = T_H - (T_H - T_{8M}) \frac{x}{x_0} \quad (52)$$

since;

$$q_{8H}(x) = C_P \dot{M} \frac{dT_{8H}(x)}{dx} \quad (53)$$

$$q_{8H}(x) = - \frac{C_P \dot{M} (T_H - T_{8M})}{x_0} \quad (54)$$

In this Configuration, the conditions are imposed that the hot and cold side media exit temperatures are the same, and that both media have the same heat capacity and flow rates. The cold side medium convects waste thermal power $q_{8C}(x)$ from the cold side. Its initial temperature is T_C ;

$$q_{8C}(x) = T_{8M} \dot{M} \frac{dT_{8C}(x)}{dx} \quad (55)$$

The power produced at location x is;

$$p_8(x) = q_{8H}(x)\eta\left(\frac{T_{8H}(x) - T_{8C}(x)}{T_{8H}(x)}\right) \quad (56)$$

The temperature profile $T_{8C}(x)$ is found from;

$$q_{8H}(x) = q_{8C}(x) + p_8(x) \quad (57)$$

Substituting values from Equations (52), and (54) to (56) into (57). The result is a first order differential equation with the solution;

$$T_{8C}(x) = T_H - (T_H - T_{8M})\frac{x}{x_0} - T_C\left(\left(1 - \frac{x}{x_0}\right)\frac{T_H}{T_{8M}} + \frac{x}{x_0}\right)^\eta \quad (58)$$

Since, by definition;

$$T_{8C}(0) = T_{8M} \quad (59)$$

Where T_{8M} satisfies the relationship;

$$\left(\frac{T_H - T_{8M}}{T_{8M} - T_C}\right) = \left(\frac{T_H}{T_{8M}}\right)^\eta \quad (60)$$

Note that the efficiency;

$$\frac{P_8}{Q_{8H}} = \frac{Q_{8H} - Q_{8C}}{Q_{8H}} \quad (61)$$

Becomes;

$$\frac{P_8}{Q_{8H}} = \frac{T_H + T_C - 2T_{8M}}{T_H - T_C} \quad (62)$$

The maximum efficiency is found by first numerically solving for T_{8M} in Equation (60), and using the result in Equation (62) to compute efficiency. Results are given in Figure 8B.

The maximum efficiency of Configuration 8 is best approximated by an altogether different methodology than that used to compute the exact solution. For relatively low efficiency systems, $T_{8H}(x)$ is essentially linear. If it is assumed that T_{8M} is approximated by;

$$T_{8M} \approx \frac{T_H + T_C}{2} \quad (63)$$

And $T_{8C}(x)$ is linearized;

$$T_{8C}(x) \approx \frac{T_H + T_C}{2} - \left(\frac{T_H - T_C}{2}\right)\frac{x}{x_0} \quad (64)$$

Equations (52), (54) and (64) can be used in Equation (56) to approximate $P_8(x)$. This can then be integrated to find an approximation for the maximum efficiency. The result is;

$$\frac{P_8}{Q_{8H}} \approx \frac{\eta}{2} \ln\left(\frac{2T_H}{T_{8M} + T_C}\right) \quad (65)$$

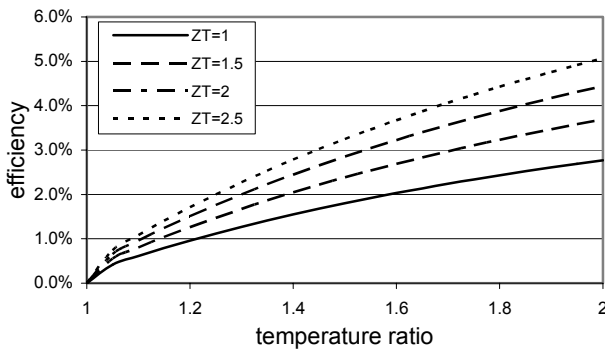


Figure 8B

This approximation is within 3% of the exact results for the range of parameters in Figure 8B.

Configuration 9

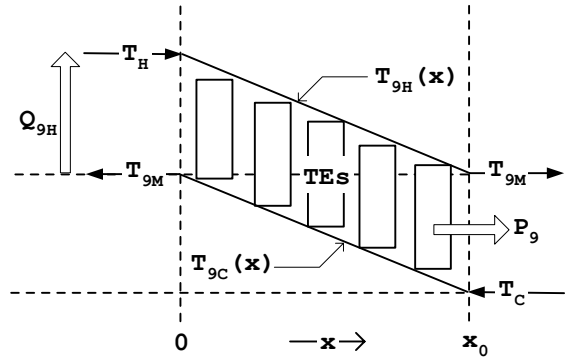


Figure 9A

Configuration 9 shown in Figure 9A is very similar to 8 except the waste cold side heat flux exiting at temperature T_{9M} is further heated to T_H and therefore, the total input power Q_{9H} becomes;

$$Q_{9H} = C_p \dot{M}(T_H - T_{9M}) \quad (66)$$

The temperature profile $T_{9C}(x)$ is the same as that of Equation (58) Configuration 8 and the power is the same as Equation (56). Thus, the maximum efficiency has the same numerator as Equation (62) and the denominator is replaced by Equation (66);

$$\frac{P_9}{Q_{9H}} = \frac{\int_0^{x_0} p_9(x) dx}{C_p \dot{M}(T_H - T_{9M})} \quad (67)$$

The maximum efficiency is computed numerically as was done with Configuration 8. Results are presented in Figure 9B. Similarly, the approximation, using a linearized $T_{9C}(x)$ yields;

$$\frac{P_9}{Q_{9H}} = \eta \ln \frac{2T_H}{T_H + T_C} \quad (68)$$

and shows the factor of two improvement over Configuration 8 as expected.

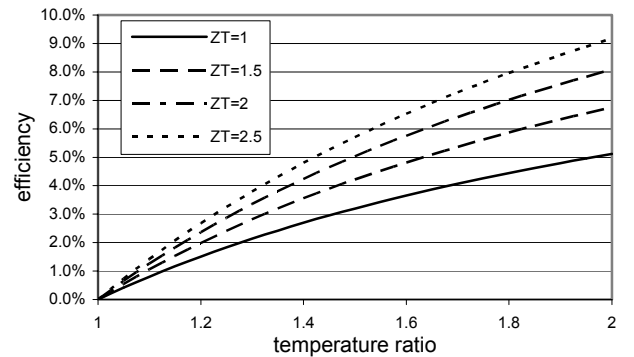


Figure 9B

Configuration 10

Configuration 10, shown in Figure 10A, is a variant on Configurations 8 and 9, again with thermally isolated TE elements where the hot side medium is at initial temperature T_G that is hotter than T_H . Heated exhaust convective medium

from the cold side can be further heated by and combined with, the hot side medium to produce a larger amount of hot side media. If both media have the same thermal capacity, the hot side heat excess content Q_{10H} is;

$$Q_{10H} = C_p \dot{M}_{10G} (T_G - T_H) \quad (69)$$

And the amount of heat Q_{10R} required to bring the cold side waste to T_H is;

$$Q_{10R} = C_p \dot{M}_{10C} (T_H - T_{10M}) \quad (70)$$

Where \dot{M}_{10G} and \dot{M}_{10C} are the hot and cold source flow rates, respectively.

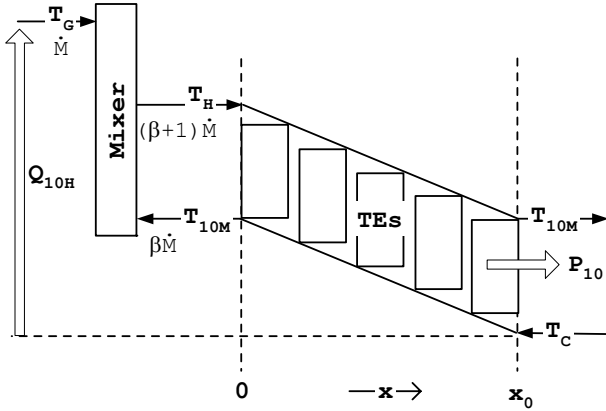


Figure 10A

Define;

$$\beta = \frac{\dot{M}_{10C}}{\dot{M}_{10G}} \quad (71)$$

Then, equating Equations (69) and (70) and using Equation (71) to eliminate \dot{M}_{10C} ;

$$\beta = \frac{T_G - T_H}{T_H - T_{10M}} \quad (72)$$

In this Configuration, let the hot side medium flow rate \dot{M}_{10H} be the combined flow rate from the hot side source \dot{M}_{10G} and the cold side exhaust \dot{M}_{10} , then;

$$\dot{M}_{10H} = (\beta + 1) \dot{M}_{10G} \quad (73)$$

$$\dot{M}_{10C} = \beta \dot{M}_{10G} \quad (74)$$

Using the process to solve for T_{10M} as was done in Equation (60);

$$T_{10G}(x) = AT_H - (AT_H - T_{10M}) \frac{x}{x_0} \left(\frac{T_H(1 - \frac{x}{x_0}) + T_{10M} \frac{x}{x_0}}{T_H} \right)^{\frac{\beta+1}{\beta} \eta} \quad (75)$$

Where;

$$A = \frac{(1-\eta)(1+\beta)}{(1-\eta)\beta - \eta} \quad (76)$$

And evaluating Equation (75) at $x = 0$ yields;

$$\left(\frac{AT_H - T_{10M}}{AT_{10M} - T_C} \right) = \left(\frac{T_H}{T_{10M}} \right)^{\frac{\beta+1}{\beta} \eta} \quad (77)$$

Again following the process for Configuration 8, Equation (77) can be solved numerically for T_{10M} and the maximum efficiency can be computed. The results are given in Figure 10B as a function of β for $T_H/T_C = 2$.

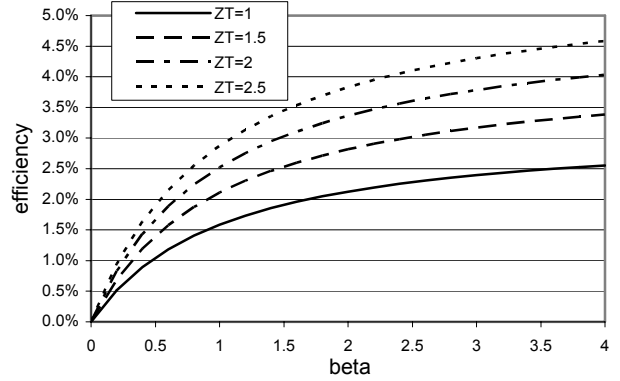


Figure 10B

Configurations 11 and 12 each utilize the energy conversion capabilities of TEs in two complementary thermodynamic cycles, and as such, are examples of a family of co-generation cycles that employ thermoelectrics. The governing equations have been presented in a previous paper [4] that laid out the general principles for TE-based co-generation systems.

In the Configurations that follow, the first generator utilizes convective flow to directly provide electric power and provide a source of convective medium at temperature T_H . Here it is sufficient to note that the convective medium absorbs thermal power from the first generator as it produces electrical power, P_{TE1} . The second generator converts a portion of the convective medium's thermal power to electric power, P_{TE2} , by employing one of the configurations discussed above.

Configuration 11

Configuration 11 is shown in Figure 11A. Convective medium enters the first generator at temperature T_C and exits at temperature T_H . The heated medium transfers thermal power to a second cycle as it cools back to T_C . The second cycle is Configuration 7. The cold side is held at constant temperature T_C . The optimum efficiency, computed numerically, is plotted in Figure 11B. In comparison to Configuration 7, the efficiency of the co-cycle generator for

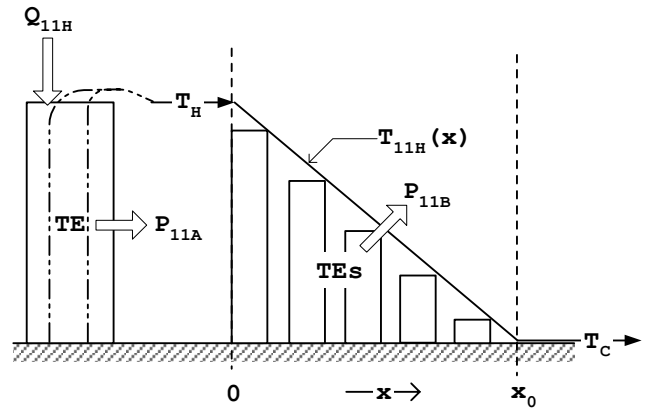


Figure 11A

the parameter range in this study is 60% to 70% higher.

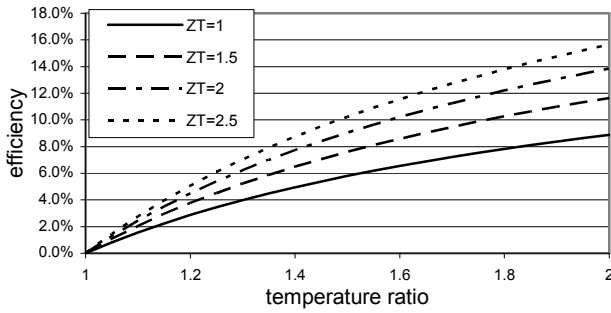


Figure 11B

Configuration 12

Configuration 12 is shown in Figure 12A. The first cycle is again a convective cycle that utilizes the heated cold side medium that exits a generator in the form of Configuration 9. Prior to entering the convective generator, the cold side medium is heated from its exit temperature T_{M1} to T_{M2} by the waste heat from the cold side of the convective generator. The medium is then heated to T_H by the convective generator. The medium completes its circuit by providing thermal power to the isolated element TE generator of Configuration 9.

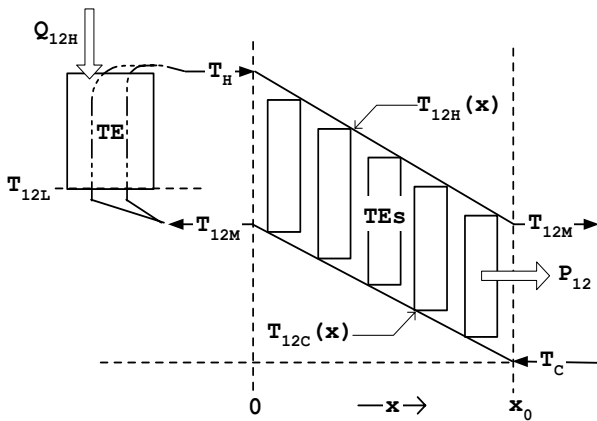


Figure 12A

Figure 12B presents the optimum efficiencies computed numerically for Configuration 12. The results show an improvement of 25% to 35% over Configuration 9.

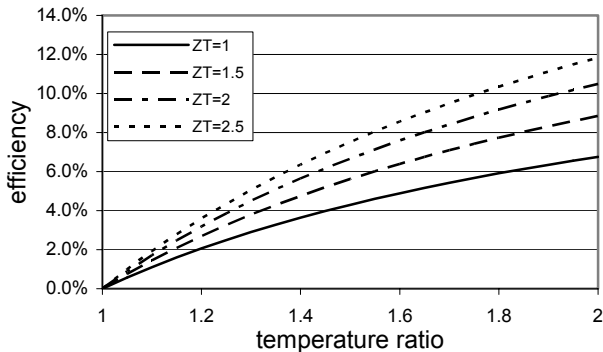


Figure 12B

Summary and Conclusions

The prospect of more efficient thermoelectric materials has led to renewed interest in solid-state waste power recovery. However, the mathematical models for computing efficiency given in most texts do not directly apply to important applications, including power recovery from automotive exhaust waste incineration and other uses where the thermal power is contained in a convective medium and from which a large fraction of the thermal power is to be extracted. In such cases, thermodynamic cycles that employ thermal isolation and convective enhancement are beneficial, especially where co-cycle generation is possible.

Table 3 presents a compilation of the results of the 12 configurations discussed above. Efficiencies are given at $T_H / T_C = 1.5$ for values of ZT_H ranging from that of today's best commercial materials to values possible over the next several years.

Configuration	ZT=1,	ZT=1,	ZT=2,	ZT=2,
	$T_H=450K$	$T_H=600K$	$T_H=450K$	$T_H=600K$
1	5.840%	8.856%	9.175%	15.841%
2	1.770%	3.039%	2.781%	4.791%
3	2.963%	4.531%	4.698%	7.243%
4	0.812%	1.268%	1.288%	2.033%
5	1.122%	1.816%	1.772%	2.889%
6	2.949%	4.497%	4.661%	7.156%
7	3.312%	5.435%	5.204%	8.569%
8	1.801%	2.773%	2.855%	4.443%
9	3.199%	5.116%	5.030%	8.083%
10	2.876%	4.023%	4.523%	6.363%
11	5.798%	8.881%	9.046%	13.841%
12	4.301%	6.755%	6.662%	10.493%

Table 3

Under conditions where the thermal flux undergoing power conversion is a small fraction of the available thermal power, or where the source is from isotope decay, solar power, or the like, and the waste side heat sink is of large capacity, standard equations apply and relatively high efficiencies can be achieved. The standard geometry and of Configuration 1 apply to these conditions. Configurations 2, 3, 4 and 5 apply where convective media are employed as the heat source and the cold side heat removal system. In these Configurations, the entire hot and cold sides of the TE converter are at uniform temperatures. The resultant system efficiencies are very low, ranging from about 12% to 33% of the standard model. These reduced efficiencies have discouraged applications of TE converters in automotive [7-9] and other important usages.

Configurations 6, 7, 8, 9 and 10 incorporate thermal isolation of TE elements to enhance efficiency for systems with convective media as sources of thermal power and heat removal. Efficiencies range from 28% to 60% of the standard system. These Configurations are easily manufactured and represent effective means of improving performance beyond that achievable with the uniform temperature hot and cold side geometries, and convective media for heating and cooling.

Configurations 11 and 12 represent co-generation systems, with the heat source being a convective medium.

Both employ convective TE cycles to enhance efficiency, and represent the highest degree of manufacturing complexity. In applications with heat sources that do not allow Configuration 1 to be utilized, these offer efficiencies of 57% to 98% of Configuration 1, for the range of conditions of this paper.

Other co-generator systems that combine solid-state electrical power production with cycles with mechanical outputs such as gasoline engines, turbine and other heat engines, are not within the scope of this paper, can have combined efficiencies above those presented here [4] but are not completely solid-state and lose the benefits associated with purely solid-state systems.

Configurations 10, 11 and 12 are representative of electrical generators that can use a combustion process, such as a catalytic burner, as a heat source. For example, air and possibly gaseous or liquid fuel can be the cold side convective media, and after combustion, provide the source of heat on the hot side. Such systems could be used as compact, simple generators. With further efficiency improvements, such TE generators using thermal isolation and convective co-generation could lead to the broader acceptance of solid power generators in both military and commercial applications.

Acknowledgements

The author is indebted to several colleagues; Ms. Janice Garcia for helpful assistance and document preparation; Mr. Ye Li for suggestions, proofreading and document preparation; Mr. Robert Diller for consultation and experimental verification; and Mr. Dylan Owens for extensive review, figure preparation and simulations.

References

1. Venkatasubramanian, R., et al, "Thin-Film Thermoelectric Devices With High Room-Temperature Figures Of Merit," *Nature*, vol. 413, (2001), pp. 597-602.
2. Harman, T.C., oral presentation, DARPA/ONR/DOE Thermoelectric Workshop, San Diego, CA.
3. Bell, L.E., "Use of Thermal Isolation to Improve Thermoelectric System Operating Efficiency," *Proceedings 21st ICT*, Long Beach, CA, August 2002.
4. Bell, L.E., "Increased Thermoelectric System Thermodynamic Efficiency by Use of Convective Heat Transport," *Proceedings 21st ICT*, Long Beach, CA, August 2002.
5. Diller, Robert W., Chang, Yu-Wen, "Experimental Results Confirming Improved Performance of Systems Using Thermal Isolation," *Proceedings 21st ICT*, Long Beach, CA, August 2002.
6. Angrist, Stanley W., Direct Energy Conversion, Third Edition, Allyn and Bacon, Inc. (Boston, 1976). Chapter 4, pp. 140-165.